Probing early-time longitudinal dynamics with the hyperon's spin polarization in relativistic heavy-ion collisions

Sangwook Ryu   Vahidin Jupic   Chun Shen

arxiv.org/pdf/2106.08125

Heavy-Ion Collision Phenomenology Journal Club
Feb 16 , 2026

Abstract

1. Λ hyperon polarisation sensitivity to study initial longitudinal dynamics.
2. Λ hyperon's global polarisation and slope of pion's directed flow can constrain the size of longitudinal flow.
3. Give size of longitudinal flow as a function of collision energy.
4. Study effects of hydrodynamic gradients like $\nabla(\mu_B/T)$ on polarisation of Λ and $\bar{\Lambda}$.

Motivation

1. Medium carrying OAM of order 10^3–$10^4\hbar$ in non-central collisions.
2. Local fluid vorticity can orient the spin of emitted particles through spin orbit coupling.
3. Parametrize the local flow by introducing fraction $(0-1)$. Λ hyperons' polarization and pion's directed flow have strong constrain on f.

About the paper:

1. Theoretical framework
   1.1 Mapping initial condition $\rightarrow$ conservation laws $\rightarrow$ with this new parameter
   1.2 Hydrodynamic evolution
   1.3 Vorticity
   1.4 Average spin vector $\leftrightarrow$ polarisation
2. Results $\rightarrow$ polarization
3. Conclusion

Theoretical framework
Mapping initial-state orbital angular momentum (OAM) to hydrodynamic fields

- Nucleon position and momentum $\{x_i^\mu, p_i^\mu\}$ from initial collision geometry (3D MC-Glauber model):
$$L^{\alpha\beta} = x^\alpha p^\beta - x^\beta p^\alpha$$
- OAM density of the fluid:
$$L^{\mu,\alpha\beta} = x^\alpha T^{\mu\beta} - x^\beta T^{\mu\alpha}$$
- Total OAM on a hypersurface:
$$L_{\text{fluid}}^{\alpha\beta} = \int d^3\sigma_\mu \, L^{\mu,\alpha\beta} = \int \tau \, dx \, dy \, d\eta_s \, L^{\tau,\alpha\beta}$$
- Local energy–momentum matching on the transverse plane ensures OAM conservation:
$$L_{\text{init}}^{\alpha\beta} = L_{\text{fluid}}^{\alpha\beta}(\tau_0)$$

The area density of energy and longitudinal momentum at a given transverse position is given by

$$\frac{d}{d^2 x_T} E(x, y) = \left[T_A(x, y) + T_B(x, y) \right] m_N \cosh(y_{\mathrm{beam}}) \equiv M(x, y) \cosh(y_{\mathrm{CM}}),$$

$$\frac{d}{d^2 x_T} P_z(x, y) = \left[T_A(x, y) - T_B(x, y) \right] m_N \sinh(y_{\mathrm{beam}}) \equiv M(x, y) \sinh(y_{\mathrm{CM}}).$$

The colliding nucleus A as the projectile with positive rapidity, while nucleus B is the target flying toward the $-z$ direction.
Here $T_{A(B)}(x, y)$ is the participant thickness function in the transverse plane, m_N is the nucleon mass, and

$$y_{\mathrm{beam}} = \operatorname{arcosh}\left(\frac{\sqrt{s_{NN}}}{2 m_N} \right).$$

The invariant mass and center-of-mass rapidity are

$$M(x, y) = m_N \sqrt{T_A^2 + T_B^2 + 2 T_A T_B \cosh(2 y_{\mathrm{beam}})},$$

$$y_{\mathrm{CM}}(x, y) = \operatorname{arctanh}\left[\frac{T_A - T_B}{T_A + T_B} \tanh(y_{\mathrm{beam}}) \right].$$

Energy–momentum conservation at each transverse position

$$
\begin{aligned}
M(x,y)\cosh\left[y_{\rm CM}(x,y)\right] &= \int d^3\Sigma_\mu\, T^{\mu t}(x,y,\eta_s) \\
&= \int \tau_0\, d\eta_s \Big[T^{\tau\tau}(x,y,\eta_s)\cosh(\eta_s) + \tau_0\; T^{\tau\eta}(x,y,\eta_s)\sinh(\eta_s)\Big], \\
M(x,y)\sinh\left[y_{\rm CM}(x,y)\right] &= \int d^3\Sigma_\mu\, T^{\mu z}(x,y,\eta_s) \\
&= \int \tau_0\, d\eta_s \Big[T^{\tau\tau}(x,y,\eta_s)\sinh(\eta_s) + \tau_0\; T^{\tau\eta}(x,y,\eta_s)\cosh(\eta_s)\Big].
\end{aligned}
$$

On the constant proper-time hypersurface $\tau = \tau_0$, assume the form

$$
\begin{aligned}
T^{\tau\tau}(x,y,\eta_s) &= e(x,y,\eta_s)\cosh(y_L), \\
T^{\tau\eta}(x,y,\eta_s) &= \frac{1}{\tau_0}\, e(x,y,\eta_s)\sinh(y_L),
\end{aligned}
$$

and neglect transverse expansion,

$$
T^{\tau x} = T^{\tau y} = 0 \qquad \text{at } \tau = \tau_0.
$$

The longitudinal flow rapidity is parameterized as

$$
y_L = f\, y_{\rm CM}, \qquad f \in [0,1].
$$

→ **Longitudinal momentum fraction** f

- Controls the size of the initial longitudinal flow
- Net longitudinal momentum of hydrodynamic fields kept fixed

→ **Energy–momentum conservation at fixed** (x, y)

$$M(x,y) = \int \tau_0 \, d\eta_s \; e(x,y,\eta_s) \, \cosh(y_L + \eta_s - y_{\rm CM}),$$
$$0 = \int \tau_0 \, d\eta_s \; e(x,y,\eta_s) \, \sinh(y_L + \eta_s - y_{\rm CM})$$

→ **Symmetric rapidity profile about** $(y_{\rm CM} - y_L)$

$$e(x,y,\eta_s) = \mathcal{N}_e(x,y) \, \exp\left[-\frac{(|\eta_s - (y_{\rm CM} - y_L)| - \eta_0)^2}{2\sigma_\eta^2}\right] \theta(|\eta_s - (y_{\rm CM} - y_L)| - \eta_0)$$

→ **Parameters**

- η_0: plateau width $\qquad$ σ_η: edge fall-off

→ **Normalization fixed by local invariant mass**

$$\mathcal{N}_e(x,y) = \frac{M(x,y)}{2\sinh(\eta_0) + \sqrt{\frac{\pi}{2}}\,\sigma_\eta \, e^{\sigma_\eta^2/2}\, C_\eta}, \qquad C_\eta = e^{\eta_0}\,\mathrm{erfc}\Big(-\tfrac{1}{\sqrt{2}\sigma_\eta}\Big) + e^{-\eta_0}\,\mathrm{erfc}\Big(\tfrac{1}{\sqrt{2}\sigma_\eta}\Big)$$

Initial energy density distributions in the $x - \eta_s$ plane for the new parameter f

- $f = 0$: local net longitudinal momentum shifts the energy-density flux tube toward forward rapidity
- $f = 1$: longitudinal momentum $P_z(x, y)$ is fully attributed to longitudinal flow velocity
- Parameter f has negligible impact on global observables (particle yields, mean p_T, v_2 at midrapidity)

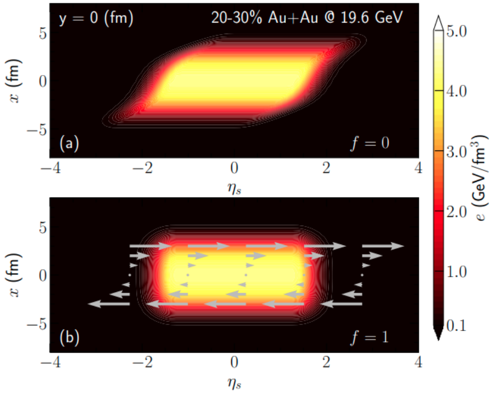

FIG. 1. Color contours show the initial energy density distributions in the $x - \eta_s$ plane for 20-30% Au+Au collisions at 19.6 GeV with the longitudinal rapidity fraction $f = 0$ (a) and $f = 1$ (b). The grey arrows in panel (b) indicate the non-zero initial longitudinal flow u^η with $y_L = y_{\rm CM}$ in Eqs. (13) and (14). $u^\eta = 0$ in panel (a).

The net-baryon number density current has the form

$$J_B^\mu(x, y, \eta_s) = n_B(x, y, \eta_s)\, u^\mu(x, y, \eta_s).$$

$$n_B(x, y, \eta_s) = T_A(x, y)\, f_{n_B}^A(\eta_s) + T_B(x, y)\, f_{n_B}^B(\eta_s).$$

$$f_{n_B}^A(\eta_s) = \mathcal{N}_{n_B}\left[\theta(\eta_s - \eta_{B,0}) \exp\left(-\frac{(\eta_s - \eta_{B,0})^2}{2\sigma_{B,\mathrm{out}}^2}\right) + \theta(\eta_{B,0} - \eta_s) \exp\left(-\frac{(\eta_s - \eta_{B,0})^2}{2\sigma_{B,\mathrm{in}}^2}\right)\right]$$

$$f_{n_B}^B(\eta_s) = \mathcal{N}_{n_B}\left[\theta(\eta_s + \eta_{B,0}) \exp\left(-\frac{(\eta_s + \eta_{B,0})^2}{2\sigma_{B,\mathrm{in}}^2}\right) + \theta(-\eta_{B,0} - \eta_s) \exp\left(-\frac{(\eta_s + \eta_{B,0})^2}{2\sigma_{B,\mathrm{out}}^2}\right)\right]$$

The relevant parameters $\eta_{B,0}$, $\sigma_{B,\mathrm{in}}$, and $\sigma_{B,\mathrm{out}}$ are determined such that the net-proton rapidity distribution is reproduced.

Hydrodynamic evolution → *MUSIC* → ($\partial_\mu T^{\mu\nu} = 0 \qquad \partial_\mu J^\mu_B = 0$)

→ Energy–momentum tensor

$$T^{\mu\nu} = e\, u^\mu u^\nu - (P + \Pi)\,\Delta^{\mu\nu} + \pi^{\mu\nu}, \qquad \Delta^{\mu\nu} = g^{\mu\nu} - u^\mu u^\nu,\; g^{\mu\nu} = \mathrm{diag}(1, -1, -1, -1)$$

→ Where, local energy density e, pressure P, fluid velocity u^μ, shear stress tensor $\pi^{\mu\nu}$, and bulk viscous pressure Π

→ Hydrodynamic equations solved with lattice-QCD-based equation of state at finite baryon density (NEOS–BQS)

- strangeness neutrality imposed
- electric charge density $n_Q = 0.4\, n_B$

→ In this work: bulk viscosity neglected ($\Pi = 0$) and no net-baryon diffusion effects

→ Shear stress tensor evolution

$$\tau_\pi D\pi^{\mu\nu} + \pi^{\mu\nu} = 2\eta\,\sigma^{\mu\nu} - \delta_{\pi\pi}\pi^{\mu\nu}\theta + \phi_7\pi_\alpha^{\langle\mu}\pi^{\nu\rangle\alpha} - \tau_{\pi\pi}\pi_\alpha^{\langle\mu}\sigma^{\nu\rangle\alpha} + \lambda_{\pi\Pi}\Pi\sigma^{\mu\nu}$$

→ Definitions: $D = u^\alpha\partial_\alpha$ (comoving derivative), $\nabla^\mu = \Delta^{\mu\alpha}\partial_\alpha$,

$$\sigma^{\mu\nu} = \tfrac{1}{2}(\nabla^\mu u^\nu + \nabla^\nu u^\mu) - \tfrac{1}{3}\Delta^{\mu\nu}(\nabla\cdot u)$$

→ Transport coefficients: shear viscosity η, relaxation time τ_π, temperature- and μ_B-dependent $(\eta/s)(T, \mu_B)$ constrained by elliptic flow in RHIC BES

Hydrodynamic vorticity

→ During hydrodynamic simulations, the fluid kinematic vorticity tensor:

$$\omega_K^{\mu\nu} = \frac{1}{2}\left(\partial^\nu u^\mu - \partial^\mu u^\nu\right)$$

→ Transverse kinematic vorticity tensor with spatial projection:

$$\omega_{K,\perp}^{\mu\nu} \equiv \frac{1}{2}\left(\nabla^\nu u^\mu - \nabla^\mu u^\nu\right)$$

→ Difference between transverse and kinematic vorticity due to local acceleration:

$$\omega_{K,\perp}^{\mu\nu} = \omega_K^{\mu\nu} - \frac{1}{2}\left(u^\nu D u^\mu - u^\mu D u^\nu\right)$$

→ Thermal vorticity:

$$\omega_{\mathrm{th}}^{\mu\nu} = \frac{1}{2}\left[\partial^\nu\left(\frac{u^\mu}{T}\right) - \partial^\mu\left(\frac{u^\nu}{T}\right)\right]$$

$$= \frac{1}{T}\left\{\omega_K^{\mu\nu} - \frac{1}{2T}\left[(\partial^\nu T)u^\mu - (\partial^\mu T)u^\nu\right]\right\}$$

→ T-vorticity:

$$\omega_T^{\mu\nu} = \frac{1}{2}\left(\partial^\nu(Tu^\mu) - \partial^\mu(Tu^\nu)\right)$$

$$= T\left\{\omega_K^{\mu\nu} + \frac{1}{2T}\left[(\partial^\nu T)u^\mu - (\partial^\mu T)u^\nu\right]\right\}$$

→ Thermal and T-vorticity receive opposite contributions from temperature gradient terms

Evolution of the fluid vorticity near midrapidity

- $\rightarrow$ Collision impact parameter is defined along the $+x$ direction
- $\rightarrow$ Global (OAM) points to the $-y$ direction
- $\rightarrow$ Λ hyperon global polarization is defined as the polarization component along the global OAM direction
- $\rightarrow$ Global polarization is related to the xz component of the thermal vorticity tensor $\omega_{\rm th}^{\mu\nu}$
- $\rightarrow$ Study the time evolution of $\omega_{\rm th}^{xz}$ during hydrodynamic evolution
- $\rightarrow$ Thermal vorticity is averaged over a given space–time volume weighted by the local energy density

$$\langle \omega_{\rm th}^{\mu\nu} \rangle (\tau) = \frac{\displaystyle\int_{\eta_s^{\rm min}}^{\eta_s^{\rm max}} d\eta_s \int d^2x_\perp \; e\, \omega_{\rm th}^{\mu\nu}}{\displaystyle\int_{\eta_s^{\rm min}}^{\eta_s^{\rm max}} d\eta_s \int d^2x_\perp \; e}$$

- $\rightarrow$ For midrapidity fluid cells, a symmetric space–time rapidity window is chosen

$$\eta_s^{\rm min} = -0.5, \qquad \eta_s^{\rm max} = 0.5$$

- $\rightarrow$ Longitudinal rapidity fraction parameter f controls how much of the global OAM is attributed to the initial local fluid vorticity
- $\rightarrow$ The initial averaged fluid vorticity $\langle \omega_{\rm th}^{\mu\nu} \rangle$ shows a good linear dependence on the model parameter f

Evolution of vorticity tensor

→ $f = 0$

- All OAM from shifts of energy-density flux tubes along η_s
- Initial fluid vorticity $\omega^{xz}_{\rm th} = 0$
- Rapid rise in first 1 fm/c, saturation at $\sim 10^{-4}$

→ Pressure gradients generate vorticity within $\sim 1\ \mathrm{fm}/c$, but magnitude is small at 200 GeV

→ $f \neq 0$

- Fraction of OAM assigned to initial fluid vorticity
- $\langle \omega^{xz}_{\rm th} \rangle$ decreases monotonically with τ

→ Different time evolution for $f = 0$ vs $f \neq 0$ indicates dominance of initial longitudinal flow distribution

→ Centrality dependence

- Larger initial vorticity in peripheral collisions
- Due to larger $T_A - T_B$ asymmetry
- Similar time evolution for all centralities

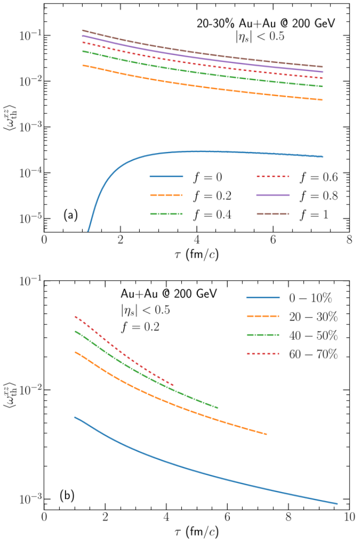

FIG. 2. (Color online) Panel (a): Time evolution of the averaged thermal vorticity of fluid with different longitudinal rapidity fraction f in mid-rapidity 20-30% Au+Au collisions at 200 GeV. Panel (b): Time evolution of the averaged thermal vorticity of fluid for four centrality bins in Au+Au collisions at 200 GeV with $f = 0.2$.

The averaged spin vector of fermions

→ Spin-1/2 average spin vector (Pauli–Lubanski) on Σ_μ:

$$S^\mu(p^\mu) = \frac{1}{4m} \frac{\int d^3\Sigma_\alpha\, p^\alpha\, \mathcal{A}^\mu}{\int d^3\Sigma_\alpha\, p^\alpha\, n_0(E)}$$

$$\mathcal{A}^\mu = \beta n_0(E)(1-n_0(E))\, \epsilon^{\mu\nu\alpha\gamma}\left[-\frac{1}{2\beta} p_\nu \omega^{\rm th}_{\alpha\gamma} - \frac{b_i}{\beta E} u_\nu p_\perp^\lambda \partial_\lambda \nabla_\gamma\left(\frac{\mu_B}{T}\right) - \frac{p_\perp^2}{E} u_\nu Q_\alpha{}^\rho \sigma_{\rho\gamma}\right]$$

→ $\epsilon^{txyz} = 1$

→ $\nabla(\mu_B/T)$ term: μ_BIP

→ shear term: SIP

→ Average polarization vector in lab frame:

$$P^\mu_{\rm lab}(p^\mu) = \frac{S^\mu(p^\mu)}{\langle S \rangle}$$

→ Polarizations measured in particle local rest frame:

$$P^t(p^\mu) = \frac{p^0}{m} P^t_{\rm lab}(p^\mu) - \frac{\vec{p}\cdot \vec{P}_{\rm lab}(p^\mu)}{m} = 0$$

$$P^i(p^\mu) = P^i_{\rm lab}(p^\mu) - \frac{\vec{p}\cdot \vec{P}_{\rm lab}(p^\mu)}{p^0(p^0+m)}\, p^i$$

→ Differential polarization vs. proper time τ:

$$P^\mu_{\rm lab}(p^\mu, \tau) = \lim_{\Delta\tau\to 0} \frac{1}{\langle S \rangle} \frac{\int_\tau^{\tau+\Delta\tau} d^3\Sigma_\alpha\, p^\alpha\, \mathcal{A}^\mu}{\int_\tau^{\tau+\Delta\tau} d^3\Sigma_\alpha\, p^\alpha\, n_0(E)}$$

$$\frac{dN}{d\tau}(p^\mu, \tau) = \lim_{\Delta\tau\to 0} \frac{1}{\Delta\tau} \int_\tau^{\tau+\Delta\tau} d^3\Sigma_\alpha\, p^\alpha\, n_0(E)$$

$$P^\mu(\tau) = \frac{\int \frac{d^3p}{E} P^\mu(p^\mu,\tau) \frac{dN}{d\tau}(p^\mu,\tau)}{\int \frac{d^3p}{E} \frac{dN}{d\tau}(p^\mu,\tau)}$$

→ To study $P^\mu(\tau)$'s contribution to the total hyperon polarization, $P^\mu(\tau)$ is weighted with the number of hyperons emitted at each time step τ

$$\frac{\Delta P^\mu}{\Delta\tau}(\tau) = \frac{P^\mu(\tau)\int \frac{d^3p}{E} \frac{dN}{d\tau}(p^\mu,\tau)}{\int d\tau \int \frac{d^3p}{E} \frac{dN}{d\tau}(p^\mu,\tau)}$$

Time evolution of hyperon polarization

$\rightarrow$ $P^y(\tau)$ drops sharply during the first 0.5 fm/c

– Follows the evolution of averaged $\langle\omega_{\mathrm{th}}^{xz}\rangle$

$\rightarrow$ $P^y(\tau)$ then increases gradually

– Reaches its peak around $\tau \sim 2.5\ \mathrm{fm}/c$ $\rightarrow$ Originates from the ω^{tx} contribution

$\rightarrow$ Hyperon production is dominated by late-time emission

- Time-like surface elements enhanced by the τ factor in Cooper–Frye particlization at late time
- Most contributions to total polarization come from late hydrodynamic times
- Early-time contributions remain small

$\rightarrow$ Fluid gradient effects

- Thermal vorticity gives the dominant contribution
- (SIP) contribution is negligible
- μ_B/T gradient effects: Suppress $\bar{\Lambda}$ global polarization by an approximately constant amount
- Λ receives larger contribution from thermal vorticity than $\bar{\Lambda}$

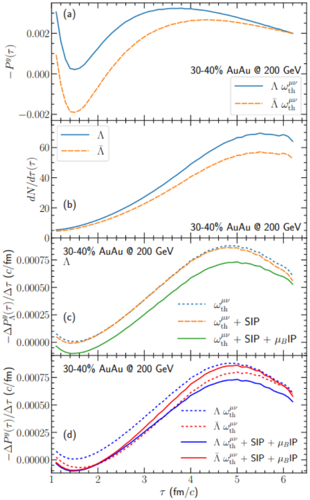

FIG. 3. (Color online) Panel (a): The hyperon's global polarization as a function of hydrodynamic proper time. Panel (b): The hyperon production as a function of τ. Panel (c): The time development of Λ's global polarization with different fluid gradients. Panel (d): The comparison of Λ and $\bar{\Lambda}$'s global polarization developments. The results are for Λ and $\bar{\Lambda}$ with $p_T \in [0.5, 3.0]$ GeV and $|y| < 1$ in 30-40% Au+Au collisions at 200 GeV with the longitudinal rapidity fraction $f = 0.2$.

POLARISATION RESULTS – f dependence

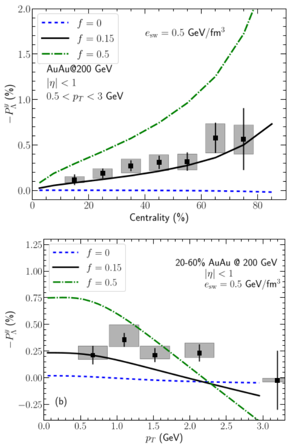

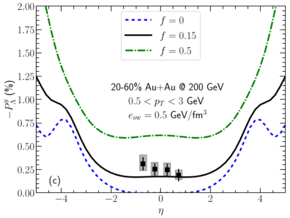

FIG. 4. (Color online) The global Λ polarization's dependence on the initial-state longitudinal rapidity fraction in Au+Au collisions at 200 GeV compared with the STAR measurements [53]. The Λ's global polarization is computed with all the gradient terms in Eq. (37). Panel (a) shows the P^y_Λ's centrality dependence. Panel (b) presents the p_T-differential P^y_Λ in 20-60% Au+Au collisions. Panel (c) shows the pseudo-rapidity dependence of P^y_Λ.

- $\rightarrow$ P^y_Λ is sensitive f. With $f = 0$, $\omega^{xz}_{\rm th} = 0 \Rightarrow$ P^y_Λ remains almost zero at midrapidity
- $\rightarrow$ $f = 0.15$ gives a good description P^y_Λ at 200 GeV. with $f = 0.5$ overestimate $\rightarrow$ factor of two
- $\rightarrow$ P^y_Λ decreases as a function of p_T. At $p_T \rightarrow 0$, the global polarization is directly related to $\omega^{xz}_{\rm th}$
- $\rightarrow$ For finite p_T, $\omega^{xz}_{\rm th}$ and $\omega^{tx}_{\rm th}$ provide additional relativistic contributions
- $\rightarrow$ $P^y_\Lambda(\eta)$ shows a plateau for $|\eta| < 2$ and different f shifts P^y_Λ by a constant.

f constrained by directed flow

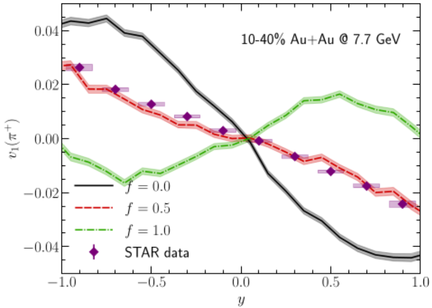

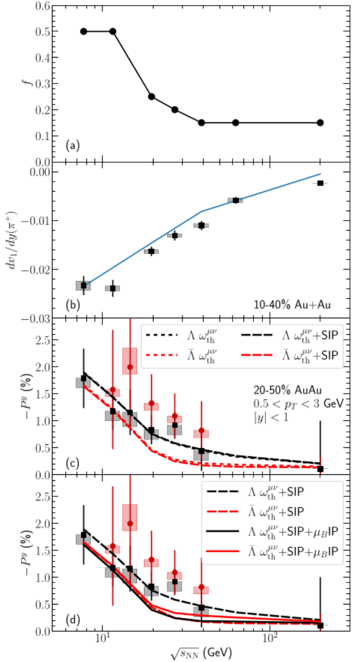

- $\rightarrow$ Large $f \Rightarrow$ small pion directed-flow slope $\left.\frac{dv_1}{dy}\right|_{y=0}$ at midrapidity
- $\rightarrow$ $f = 0.5$ preferred for Au+Au at 7.7 GeV compared with STAR data
- $\rightarrow$ Pion directed-flow slope tightly constrains f
- $\rightarrow$ f adjusted at each collision energy to match $\left.\frac{dv_1}{dy}\right|_{y=0}$. f increases from 0.15 (200 GeV) to 0.5 (7.7 GeV)

Centrality dependence

→ Model calculations describe the centrality dependence of STAR data at 200 GeV

→ μ_B-gradient–induced polarization terms reverse the difference between Λ and $\bar{\Lambda}$ global polarization

→ Net baryon density evolution and its gradients are crucial for understanding the Λ–$\bar{\Lambda}$ polarization difference

→ Prediction for Λ polarization at 7.7 GeV including all gradient terms

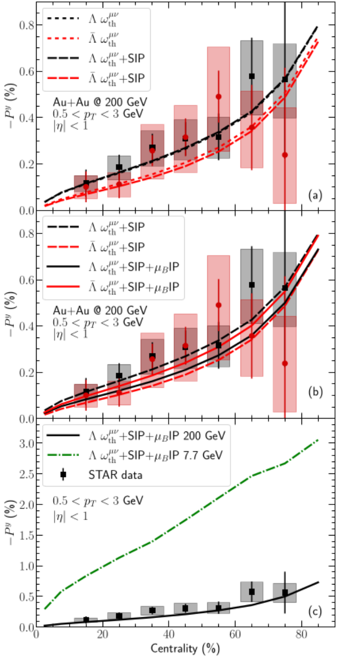

p_T and η dependence

10

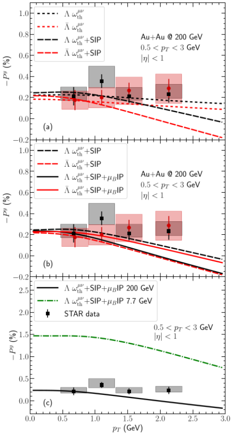

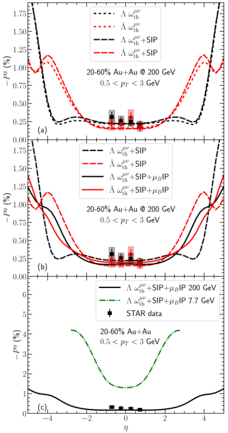

FIG. 9. (Color online) Panels (a) and (b): The p_T-differential polarization for Λ with different gradient terms in 20-60% Au+Au collisions compared with the STAR measurements [53]. Panel (c): Model prediction for $P^y_\Lambda(p_T)$ at 7.7 GeV. The STAR polarization data points are rescaled by 0.877 because the latest hyperon decay parameter α_Λ [55].

FIG. 10. (Color online) Panels (a) and (b): The pseudorapidity dependence of the Λ polarization with different gradient terms in 20-60% Au+Au collisions at 200 GeV compared with the STAR measurements [53]. Panel (c): Model prediction for $P^y_\Lambda(\eta)$ at 7.7 GeV. The STAR polarization data points are rescaled by 0.877 because the latest hyperon decay parameter α_Λ [55].

Conclusions

- $\Rightarrow$ Hybrid dynamical framework conserves energy, momentum, and orbital angular momentum (OAM) from initial geometry through hydrodynamic evolution by itroducing Longitudinal rapidity fraction parameter f.
- $\Rightarrow$ This model parameter controls the amount of fluid vorticity correlated with the initial OAM.
- $\Rightarrow$ Initial fluid vorticity strongly correlates with f at particlization and with the magnitude of global Λ polarization
- $\Rightarrow$ Pion directed flow together with global Λ polarization tightly constrains the size of initial longitudinal flow velocity across collision energies.
- $\Rightarrow$ Global Λ polarization is dominated by thermal vorticity, with shear-induced polarization affecting p_T dependence and μ_B-gradient–induced polarization modifying the Λ–$\bar{\Lambda}$ ordering